METODĂ GRAFICĂ DE PROFILARE A SCULEI DISC GENERATOARE A CANALULUI ELICOIDAL AL FREZEI DENTARE DIN CARBURĂ DE WOLFRAM

GRAPHICAL METHOD FOR PROFILING THE SIDE MILL WHICH GENERATE HELICAL FLUTE OF TUNGSTEN CARBIDE DENTAL CROSS CUT BUR

NICUȘOR BAROIU[1] * , LILIANA BAROIU[2], VIRGIL GABRIEL TEODOR[1], LUCIAN TOMA CIOCAN[3]

[1] Department of Manufacturing Engineering, "Dunărea de Jos" University of Galaţi, Domnească street, no. 47, 800201, Galați, Romania

[2] Medicine and Pharmacy Research Center, "Dunărea de Jos" University of Galati, Domnească street, no. 47, 800201, Galați, Romania

[3] Prosthetics Technology and Dental Materials Department, "Carol Davila" University of Medicine and Pharmacy, Dionisie Lupu street, no. 37, 030167, Bucharest, Romania

Super hard tungsten carbide dental fissure bur for cutting dental crowns of carbide has a longer lifetime than regular carbide millings and minimize the risk of fractures, due theirs concentricity. From the perspective of tooth geometry, in this case a smaller cutting angle, they assure a smoother and more efficient cutting.

Such geometry requires accurate, fast and efficient helical flute profiling methods of profiling, given also the diminished dimensions of such dental tools.

The profiling of side mill which generate helical flute of the dental crosscut bur may be done using analytical methods: Gohman or Nikolaev. In this paper, it is proposed a graphical method, the method of "substitutive circles" for profiling of side mill which generate a helical flute of the dental bur.

In order to prove the accuracy of the method it is proposed the check of the axial profile of the side mill by an analytical method completed with a numerical example of the form and coordinates of the tool's axial section.

The proposed method, developed in the CATIA graphical design environment is characterized by the simplicity and accuracy for profile determination.

The method is also very intuitive.

Frezele cilindrice extradure din carbură de wolfram pentru tăiat coroanele dentare au o durată de utilizare mai mare decât frezele obişnuite din carbură şi minimizează riscul de fractură datorită concetricităţii lor. Din perspectiva geometriei dinţilor, în speţă un unghi de tăiere mai mic, ele asigură o tăiere mai fină şi mai eficientă.

O astfel de geometrie necesită metode de profilare a sculei disc generatoare a canalului elicoidal precise, rapide şi eficiente, date fiind şi dimensiunile reduse ale unor astfel de scule stomatologice.

Profilarea sculei disc pentru generarea canalului elicoidal al frezei dentare se poate face utilizând metodele analitice: Gohman sau Nikolaev. În lucrare, se propune o metodă grafică, "metoda familiei de cercuri substitutive" pentru profilarea sculei disc generatoare a unui canal elicoidal, precum canalul între doi dinţi ai frezei dentare. Pentru verificarea exactităţii metodei grafice, în lucrare, se propune verificarea profilului axial al sculei disc şi printr-o metodă analitică, finalizată cu o exemplificare numerică a formei şi coordonatelor secţiunii axiale a sculei disc generatoare a canalului elicoidal al frezei dentare. Metoda grafică propusă, dezvoltată în mediul de proiectare grafică Catia, se caracterizează prin simplitatea aplicării şi o foarte mare exactitate în determinarea profilului. De asemenea, metoda este deosebit de intuitivă.

Keywords: *CAD profiling method, side mill, helical surfaces, dental bur*

1. Introduction

The mixture of metallic powder with chemical components such as wolfram, cobalt, thallium, titanium, etc., heated up until the particles adhere to one another by the synthesizing method, gives the tungsten carbide thus obtained a high hardness [1]. Under these conditions, dental cross cut bur made of such material [2] are often used in applications for the removal of ceramic and metal-ceramic crowns, as well as bridges, irrespective of the material used (porcelain, acrylate, etc.) in excavation surgeries, or even finishing and adjusting acrylic composites or other conventional fill materials [3, 4]. The instruments for dental surgery and implants include some specific tools for cleaning decay or to remove old crowns. Such tools are helical surface with constant pitch [5]. The generation of such helical surfaces with tools bounded by revolution surfaces is a

* Autor corespondent/*Corresponding author*,
E-mail: Nicusor.Baroiu@ugal.ro

particular problem.

They are known analytical methods, based on the Olivier fundamental theorem, for profiling tools which generate by enveloping, with linear contact between the enwrapping surfaces [6] or based on the theorem dedicated to these enveloping problem, the Nikolaev theorem [7, 8].

The generating tool's profiling issue, as so as, the active surfaces of cutting teeth constitute engineering concerns, some of them presented by [6] and [8], for the case of freeform surfaces, as so as, for the case of machining of helical tool's teeth [9].

Another special issue linked with enveloping helical surfaces is approached using specific mathematic means, by the analytical method of surface enveloping [10].

A particular case is the generation of helical surfaces with pre-formed tools and determining of form for surface to be generated imposing the machining path, for a tools assembly which generates successive a helical surface with complex generatrix [11].

The approach of this issue needs a specific method which simplifies the calculus, without affect the precision of generating tool's profile determination. They were elaborated some complementary analytical methods [12] as "the method of substitutive circles family" which solve the issue of side mill for generation of a cylindrical helical surface with constant pitch, transforming from a contact problem between two surfaces, in a contact problem between two curves belong to the two surfaces, simplifying the issue of side mill profiling.

Also, the developing of graphical design environments, as CATIA, allow a rigorous and fast approach for determining the profile of tool bounded by a revolution surface reciprocally enveloping with a helical surface [13, 14].

In this paper, is proposed a graphical method, based on the method of substitutive circles family, for profiling the side mill reciprocally enveloping with the flute's surface of the dental bur. The method, fast and rigorous, is developed in CATIA graphical design environment. In the same time, it is presented a numerical example, for a particular case, in order to prove the method quality.

The side mill tool's profiling (second order tool) for generating flutes of tungsten carbide dental bur for cutting dental crows assumes the following algorithm: determination of expressions of surface to be generated (this is the helical surface of the tungsten carbide dental bur's flute); determination of the enwrapping condition and finally determination of the primary peripheral surface of the second order tool, namely the side mill.

2. The surface to be generated

The helical flute of the dental bur was measured with a coordinate measuring machine Sinowon VMM-1510P, with the Quickmeasuring 32 software, see Figure 1.

The measuring of the tool's body allows obtaining its axial section. Based on the axial section was created the model of the dental bur, see Figure 2.

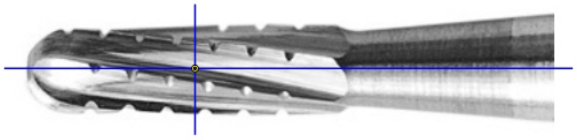

Fig. 1 - Sinowon VMM-1510P measuring – Tungsten carbide round end cross cut fissure dental bur / *Măsurarea pe maşina Sinowon VMM-1510P a frezei cilindrice cu cap rotunjit din carbură de wolfram, pentru tăiat coroane dentare.*

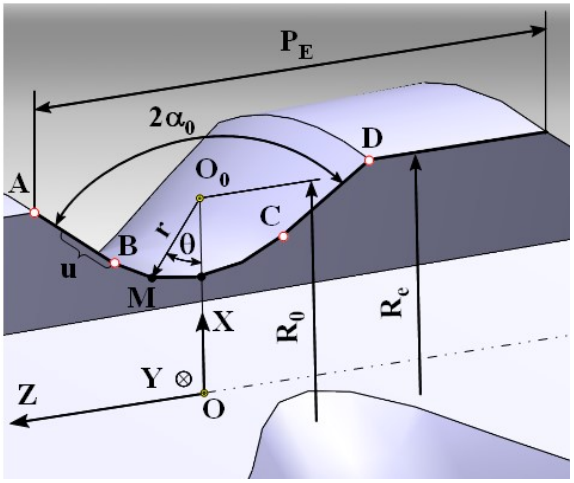

Fig. 2 - Axial section of dental crosscut bur / *Secţiunea axială a sculei elicoidale (freza dentară).*

The characteristic elements of the axial section are: R_e - external profile radius [mm]; R_o - the position of fillet center, O_o [mm]; P_E - helical pitch [mm]; $2\alpha_o$ - angle of the axial profile [^{o}]; r - fillet radius at the profile dedendum [mm].

Based on these measurements it is possible to write the specifically equations of the axial section generatrix, for a composed profile, see Figure 2.

The $\overset{\frown}{BC}$ circular arc, with radius r and θ angular parameter, has the equations:

$$\overset{\frown}{BC}\begin{vmatrix} X = R_0 - r\cdot\cos\theta; \\ Y = 0; \\ Z = r\cdot\sin\theta, \end{vmatrix} \quad (1)$$

in a reference system where the *Z* axis is overlapped to the axis of the helical surface and the *X* axis is the symmetry axis of the measured gap.

The $\overline{AB}$ straight line segment has the equations:

$$\overline{AB}\quad\begin{vmatrix} X = R_0 - r\cdot sin\,\alpha_0 + u\cdot cos\,\alpha_0; \\ Y = 0; \\ Z = r\cdot cos\,\alpha_0 + u\cdot sin\,\alpha_0, \end{vmatrix} \tag{2}$$

with *u* variable parameter.

The helical surface of the flute, for right helicoids, is described by a coordinate transformation on form:

$$\begin{pmatrix} X \\ Y \\ Z \end{pmatrix} = \begin{pmatrix} cos\,\varphi & -sin\,\varphi & 0 \\ sin\,\varphi & cos\,\varphi & 0 \\ 0 & 0 & 1 \end{pmatrix}\cdot\begin{pmatrix} X(\theta) \\ Y(\theta) \\ Z(\theta) \end{pmatrix} + \begin{pmatrix} 0 \\ 0 \\ p\cdot\varphi \end{pmatrix}, \tag{3}$$

with φ as angular parameter, variable, and *p* helical parameter,

$$p = P_E / 2\pi. \tag{4}$$

So, for the two elementary profiles, $\overline{BC}$ and $\overline{AB}$, results the equations:

$$\Sigma_{BC}\quad\begin{vmatrix} X = \left[R_0 - r\cdot cos\,\theta\right]\cdot cos\,\varphi; \\ Y = \left[R_0 - r\cdot cos\,\theta\right]\cdot sin\,\varphi; \\ Z = r\cdot sin\,\theta + p\cdot\varphi, \end{vmatrix} \tag{5}$$

with limits of θ parameter,

$$\theta_{min} = 0^o;\quad \theta_{max} = \pi/2 - \alpha\,. \tag{6}$$

Similarly:

$$\Sigma_{AB}\quad\begin{vmatrix} X = \left[R_0 - r\cdot sin\,\alpha_0 + u\cdot cos\,\alpha_0\right]\cdot cos\,\varphi; \\ Y = \left[R_0 - r\cdot sin\,\alpha_0 + u\cdot cos\,\alpha_0\right]\cdot sin\,\varphi; \\ Z = r\cdot cos\,\alpha_0 + u\cdot sin\,\alpha_0 + p\cdot\varphi, \end{vmatrix} \tag{7}$$

with limits of *u* parameter,

$$u_{min} = 0;\quad u_{max} = \frac{R_e - R_0 + r\cdot sin\,\alpha_0}{cos\,\alpha_0}. \tag{8}$$

In following, is presented an analytical method for determination of the second order side mill's primary peripheral surface.

3. Analytical method for profiling side mill which generate the helical flute

It is proposed a solution for profiling the side mill, using the Nikolaev analytical method [6, 7, 12]. The position of the future side mill axis is defined. The side mill is a tool bounded by a surface of revolution, in the reference system of the helical flute, see equations (5) and (7) and, also, the Figure 3. The axis of the side mill, $\vec{A}$, overlapped with Z_1 axis of the reference system, is disjunctive regarding the axis of the worm to be generated, $\vec{V}$, [7]. The distance between the two axis measured along the *Y* axis is denoted with "*a*" and the inclination angle between axes $\vec{V}$ and $\vec{A}$ is ω, see Figure 4.

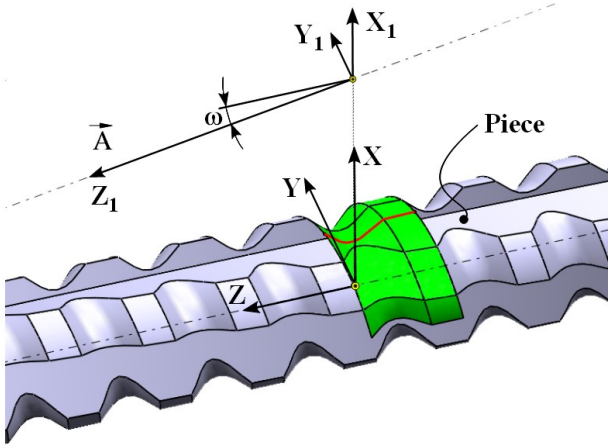

Fig. 3 - The position of the reference system joined with side mill, regarding the helix / *Poziţia axei viitoarei scule disc, în raport cu elicoidul* .

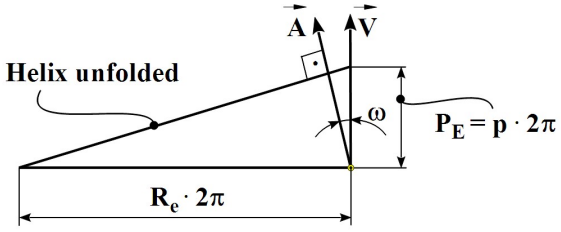

Fig. 4 - Angle between $\vec{A}$ and $\vec{V}$ axis / / *Unghiul de înclinare al axei* $\vec{A}$ *faţă de* $\vec{V}$.

The $\vec{A}$ axis is perpendicular to the cylindrical helix of the helical surface with radius R_e.

The ω angle is:

$$tg\,\omega = \frac{p}{R_e},\ p \text{ – helical parameter.} \tag{9}$$

The distance between axes,

$$a = \left(R_o - r\right) + R_{es},\ \text{see Figure 1.} \tag{10}$$

R_{es} is the external radius of the side mill, determined by technological reasons.

The Nikolaev theorem [7], [8], states that the characteristic curve between the helical surface Σ and the primary peripheral surface of the side mill, *S*, is the geometrical locus of points on the helical surface where the normals to this intersect the $\vec{A}$ axis, the axis of the future side mill (the axis of *S* surface).

In analytical form, the previous definition is given as

$$\left(\vec{N}_{\Sigma},\ \vec{A},\ \vec{r}_1\right)=0 \qquad (11)$$

where:

$\vec{N}_{\Sigma}$ is the normal to the helical surface, see Σ_{AB} and Σ_{BC};

$\vec{A}$ - the axis unit vector of the *S* revolution surface;

$\vec{r}_1$ - position vector of the current point from Σ_{AB}, Σ_{BC}, in regard to the origin of $X_1Y_1Z_1$ reference system.

The (11) condition is regarded as co-planarity condition of the three vectors, $\vec{N}_{\Sigma}$, $\vec{A}$ and $\vec{r}_1$. The characteristic curve of the surfaces *S* and Σ is the projection of the $\vec{V}$ axis onto the helical surface, here Σ_{AB} and Σ_{BC}.

The vectors which define the Nikolaev condition, $\vec{N}_{\Sigma}$, $\vec{A}$ and $\vec{r}_1$ should be regarded in the same reference system, in *XYZ* reference system.

So, the unitary vector of the $\vec{A}$ axis has the directrix cosine:

$$\vec{A}=-\sin\omega\cdot\vec{j}+\cos\omega\cdot\vec{k}. \qquad (12)$$

The $\vec{r}_1$ vector has the form

$$\vec{r}_1=\vec{r}-a\cdot\vec{i}, \qquad (13)$$

where: $\vec{r}$ is the position vector of the current point Σ_{AB}, respectively Σ_{BC}, see equations (5) and (7);

$a\cdot\vec{i}$ is the position vector of the origin of $X_1Y_1Z_1$ reference system regarding the origin of the *XYZ* reference system of the helical surface.

The calculus of normals to the helical flanks assumes the definition of the partial derivatives:

- for Σ_{BC} surface, from (5):

$$\begin{aligned}\dot{X}_{\varphi}&=-\left[R_0-r\cdot\cos\theta\right]\cdot\sin\varphi;\\ \dot{Y}_{\varphi}&=\left[R_0-r\cdot\cos\theta\right]\cdot\cos\varphi;\\ \dot{Z}_{\varphi}&=p.\end{aligned} \qquad (14)$$

and respectively,

$$\begin{aligned}\dot{X}_{\theta}&=r\cdot\sin\theta\cdot\cos\varphi;\\ \dot{Y}_{\theta}&=r\cdot\sin\theta\cdot\sin\varphi;\\ \dot{Z}_{\theta}&=r\cdot\cos\theta.\end{aligned} \qquad (15)$$

- for Σ_{AB} surface, from (7):

$$\begin{aligned}\dot{X}_{\varphi}&=-\left[R_0-r\cdot\sin\alpha_0+u\cdot\cos\alpha_0\right]\cdot\sin\varphi;\\ \dot{Y}_{\varphi}&=\left[R_0-r\cdot\sin\alpha_0+u\cdot\cos\alpha_0\right]\cdot\cos\varphi;\\ \dot{Z}_{\varphi}&=p.\end{aligned} \qquad (16)$$

and respectively,

$$\begin{aligned}\dot{X}_{u}&=\cos\alpha_0\cdot\cos\varphi;\\ \dot{Y}_{u}&=\cos\alpha_0\cdot\sin\varphi;\\ \dot{Z}_{u}&=\sin\alpha_0.\end{aligned} \qquad (17)$$

Considering the previous relations, the normal $\vec{N}_{\Sigma_{BC}}$

$$\vec{N}_{\Sigma_{BC}}=\begin{vmatrix}\vec{i} & \vec{j} & \vec{k}\\ \dot{X}_{\theta} & \dot{Y}_{\theta} & \dot{Z}_{\theta}\\ \dot{X}_{\varphi} & \dot{Y}_{\varphi} & \dot{Z}_{\varphi}\end{vmatrix} \text{ or} \qquad (18)$$

$$\vec{N}_{\Sigma_{BC}}=N_{X_{BC}}\cdot\vec{i}+N_{Y_{BC}}\cdot\vec{j}+N_{Z_{BC}}\cdot\vec{k} \qquad (19)$$

with definitions:

$$\begin{aligned}N_{X_{BC}}&=\dot{Y}_{\theta}\cdot\dot{Z}_{\varphi}-\dot{Z}_{\theta}\cdot\dot{Y}_{\varphi};\\ N_{Y_{BC}}&=-\left[\dot{X}_{\theta}\cdot\dot{Z}_{\varphi}-\dot{Z}_{\theta}\cdot\dot{X}_{\varphi}\right];\\ N_{Z_{BC}}&=\dot{X}_{\theta}\cdot\dot{Y}_{\varphi}-\dot{X}_{\varphi}\cdot\dot{Y}_{\theta},\end{aligned} \qquad (20)$$

with partial derivatives from (14) and (15) and, similarly, for Σ_{AB} with partial derivatives from (16) and (17).

In this way, the condition for determining the characteristic curve (11) may be described, for the two helical surfaces, with equations 21, 22.

The equations (21) respectively (22) together with the equations of the helical surfaces (5) respectively (7), determine the characteristic curves onto these surfaces, basically, in forms:

- for BC surface, the (21) condition represents a dependency $\varphi=\varphi(\theta)$ (23) and so, the characteristic curve is:

- for Σ_{BC} surface

$$\begin{vmatrix}\left[R_0-r\cdot\cos\theta\right]\cdot\cos\varphi-a & \left[R_0-r\cdot\cos\theta\right]\cdot\sin\varphi & r\cdot\sin\theta+p\cdot\varphi\\ N_{X_{BC}} & N_{Y_{BC}} & N_{Z_{BC}}\\ 1 & \sin\omega & \cos\omega\end{vmatrix}=0 \qquad (21)$$

- for Σ_{AB} surface

$$\begin{vmatrix} \left[R_0 - r\cdot sin\,\alpha_0 + u\cdot cos\,\alpha_0\right]\cdot cos\,\varphi & \left[R_0 - r\cdot sin\,\alpha_0 + u\cdot cos\,\alpha_0\right]\cdot sin\,\varphi - a & r\cdot cos\,\alpha_0 + u\cdot sin\,\alpha_0 + p\cdot\varphi \\ N_{X_{AB}} & N_{Y_{AB}} & N_{Z_{AB}} \\ 1 & -sin\,\omega & cos\,\omega \end{vmatrix} = 0 \quad (22)$$

$$C_{\Sigma_{BC}} \begin{vmatrix} X = X(\theta); \\ Y = Y(\theta); \\ Z = Z(\theta); \end{vmatrix} \quad (24)$$

- for AB surface, the (22) condition is $\varphi = \varphi(u)$ (25) and the characteristic curve is in form:

$$C_{\Sigma_{AB}} \begin{vmatrix} X = X(u); \\ Y = Y(u); \\ Z = Z(u). \end{vmatrix} \quad (26)$$

The equations of the characteristic curves are reported to the tool's reference system, $X_1Y_1Z_1$, by transformation, see Figure 5:

$$\begin{Vmatrix} X_1 \\ Y_1 \\ Z_1 \end{Vmatrix} = \begin{pmatrix} 1 & 0 & 0 \\ 0 & cos\,\omega & sin\,\omega \\ 0 & -sin\,\omega & cos\,\omega \end{pmatrix} \cdot \left[\begin{pmatrix} X \\ Y \\ Z \end{pmatrix} - \begin{pmatrix} a \\ 0 \\ 0 \end{pmatrix} \right] \quad (27)$$

or

$$\begin{aligned} X_1 &= X - a; \\ Y_1 &= Y\cdot cos\,\omega + Z\cdot sin\,\omega; \\ Z_1 &= -Y\cdot sin\,\omega + Z\cdot cos\,\omega. \end{aligned} \quad (28)$$

with

$$\omega = arctg\left[\frac{p/2\pi}{R_e}\right]; \quad (29)$$

$$p = \frac{P_E}{2\pi}. \quad (30)$$

In this way, in principle, the equations of the characteristic curves, in the $X_1Y_1Z_1$ reference system, have the form:

$$C_{\Sigma_{BC}} \begin{vmatrix} X_1 = X_1(\theta); \\ Y_1 = Y_1(\theta); \\ Z_1 = Z_1(\theta); \end{vmatrix} \text{ and } C_{\Sigma_{AB}} \begin{vmatrix} X_1 = X_1(u); \\ Y_1 = Y_1(u); \\ Z_1 = Z_1(u). \end{vmatrix} \quad (31)$$

By rotating the curves (31) around the $\vec{A}$ axis, with φ_1 angular parameter,

$$\begin{pmatrix} X_1 \\ Y_1 \\ Z_1 \end{pmatrix} = \begin{pmatrix} cos\,\varphi_1 & -sin\,\varphi_1 & 0 \\ sin\,\varphi_1 & cos\,\varphi_1 & 0 \\ 0 & 0 & 1 \end{pmatrix} \cdot \begin{pmatrix} X_1(\theta) \\ Y_1(\theta) \\ Z_1(\theta) \end{pmatrix} \quad (32)$$

or

$$S_{BC} \begin{vmatrix} X_1 = X_1(\theta)\cdot cos\,\varphi_1 - X_1(\theta)\cdot sin\,\varphi_1; \\ Y_1 = Y_1(\theta)\cdot sin\,\varphi_1 + Y_1(\theta)\cdot cos\,\varphi_1; \\ Z_1 = Z_1(\theta), \end{vmatrix} \quad (33)$$

results the equations of the *S* surface. The *S* surface is reciprocally enveloped with the Σ_{AB} and S_{BC} surfaces. The assembly of S_{AB} and S_{BC} surfaces represent the primary peripheral surface of the side mill.

The axial section of the S_{AB} and S_{BC} surfaces represents the profile of the secondary order tool, which generates the revolution surface, see Figure 6.

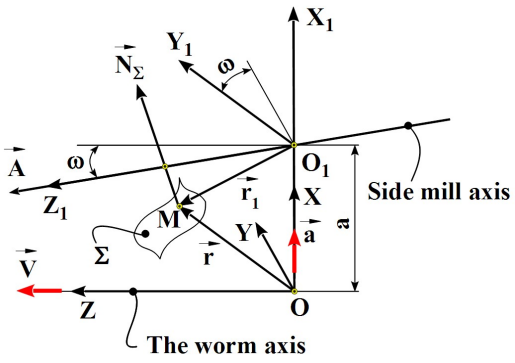

Fig. 5 - Reference systems. Geometrical form of Nikolaev condition / / *Sisteme de referinţă. Interpretarea geometrică a condiţiei Nikolaev.*

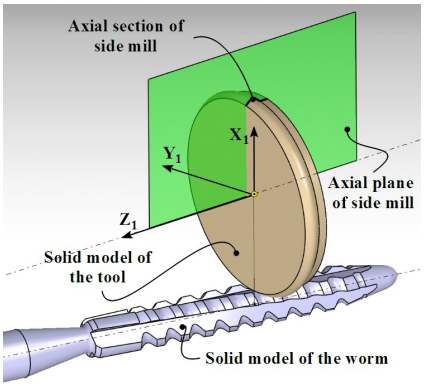

Fig. 6 - Axial section of the side mill / *Secţiunea axială a sculei disc.*

The simplest form of the axial section is obtained from the equations (31) with notations:

$$\begin{vmatrix} H = Z_1; \\ R = \sqrt{X_1^2 + Y_1^2}. \end{vmatrix} \quad (34)$$

In following, it is presented a numerical example based onto the previously presented algorithm, for the actual case showed in Table 1, see Figure 2:

Table 1

Numerical values of the helical surface parameters
Valorile numerice ale parametrilor suprafeţei elicoidale

Parameter	Value
R_e [mm]	0.882
R_o [mm]	0.661
P_E [mm]	2.138
$2\alpha_0$ [°]	96.717
r [mm]	0.268
a [mm]	5

In Table 2, are presented the coordinates of the characteristic curve onto the helical surface *Σ*.

In Figure 7, is presented the form of the axial section for the revolution surface *S,* which constitutes the primary peripheral surface of the side mill reciprocally enveloping with the helical surfaces Σ_{AB} and Σ_{BC}, see Table 2 and (28).

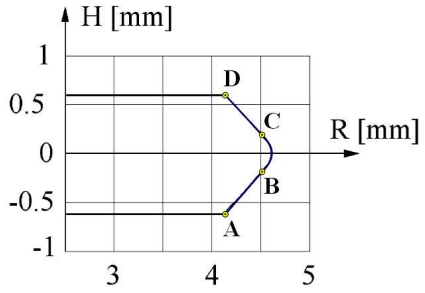

Fig. 7 - Axial section of the revolution surface / *Secţiunea axială a suprafeţei de revoluţie.*

4. Graphical method for side mill profiling

As alternative to the proposed analytical method, a graphical method was developed based on the capabilities of the computer assisted design programs.

The graphical method, developed in CATIA, for profiling the side mill reciprocally enveloping of a cylindrical helical surface with constant pitch, is based on the complementary theorem of the "family of the substitutive circles" [12]. This theorem states that: the revolution surface, which envelope a helical cylindrical surface with constant pitch, is formed by an assembly of circles, having the centers onto the revolution axis and, which, in planes perpendicularly to this axis, are tangents to the intersection curves between the helical surface and the considered planes. The theorem is illustrated in Figure 8 and Figure 9.

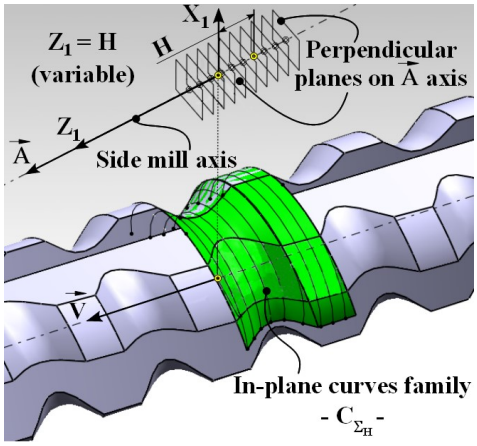

Fig. 8 - The theorem of substituting circles family: the planes family $Z_1 = H$; C_{Σ_H} curves family / / *Metoda cercurilor substitutive: familia de plane* $Z_1 = H$; *familia de curbe* C_{Σ_H}.

In planes $Z_1 = H$, (Z is overlapped to $\vec{A}$ axis of the future revolution surface) are defined the circles with radius R_H, tangents to the intersecting curves of helical surfaces with *H* planes, which define the C_{Σ_H} curves onto the helical surface to be generated. The totality of tangency points, T_H, thus defined, constitutes the common characteristic of the future revolution surface, *S*, and of the helical surface.

Table 2

Characteristic curve coordinates / *Coordonatele curbei caracteristice*

	X [mm]	Y [mm]	Z [mm]		X [mm]	Y [mm]	Z [mm]		X [mm]	Y [mm]	Z [mm]
	-0.0446	0.8732	-0.6259		-0.0991	0.4251	-0.0690		0.1193	0.4653	0.1147
	-0.0520	0.8261	-0.5695		-0.0801	0.4137	-0.0549		0.1114	0.5080	0.1714
	-0.0598	0.7793	-0.5128		-0.0608	0.4046	-0.0408		0.1029	0.5516	0.2283
	-0.0681	0.7328	-0.4561		-0.0410	0.3982	-0.0270		0.0942	0.5960	0.2852
AB	-0.0766	0.6867	-0.3992	**BC**	-0.0207	0.3943	-0.0135	**CD**	0.0853	0.6411	0.3422
	-0.0854	0.6411	-0.3422		0.0000	0.3930	0.0000		0.0766	0.6867	0.3992
	-0.0942	0.5960	-0.2852		0.0207	0.3943	0.0135		0.0680	0.7328	0.4561
	-0.1029	0.5516	-0.2283		0.0411	0.3982	0.0270		0.0598	0.7793	0.5129
	-0.1114	0.5080	-0.1714		0.0608	0.4046	0.0408		0.0520	0.8261	0.5695
	-0.1193	0.4653	-0.1147		0.0801	0.4137	0.0549		0.0446	0.8732	0.6259

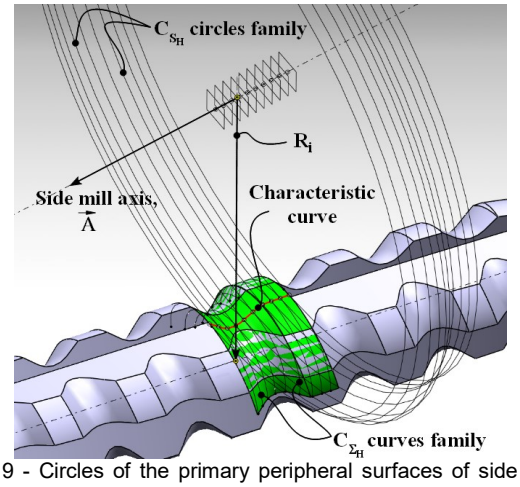

Fig. 9 - Circles of the primary peripheral surfaces of side mill; C_{Σ_H} curves family / *Cercurile suprafeței periferice primare a sculei disc; familia de curbe* C_{Σ_H} .

4.1 Graphical solution

In order to find the axial profile of the side mill, are generated in CATIA all the necessary geometrical elements. The solid modeling of the helical bur and of the reference systems associated with generated surface and with the side mill, are done using the specific commands in *Part Design and Generative Shape Design* environments.

The helical bur and the future side mill will have a contact curve called characteristic curve. To determine this curve, on the axis of side mill are selected equidistant points. For a good accuracy of profile calculus, the distances between these points have to be very small. From these points are drawn perpendicular planes to the axis. Using the *Intersection* command from the *Generative Shape Design* environment, the bur solid model is intersected with these planes, obtaining the intersection curves for each of these planes. Next, regarding the point on the axis as center, with the command *Circle*, and the option *Center and Tangent*, is constructed the tangent circle to the previously obtained curve for each plane. Afterwards, this circle is intersected with the corresponding curve and the tangency point is obtained. The geometric locus of these tangency points is the characteristic curve. Through these points is drawn a spline curve which is the characteristic curve. In the same environment, *Generative Shape Design*, using the command *Revolute*, the characteristic curve is rotate around the $\vec{A}$ axis. The revolutions surface is the primary peripheral surface of the side mill. Its axial section is obtained with the command *Intersection*. Next, points from this section are exported with a VBA application in a .txt or .xls file.

4.2 Graphical method verification

In order to prove the method quality it was made a verification using the Nikolaev condition. In each of the points belongs to the characteristic curve, it was calculated the normal direction to the helical surface, $\vec{N}_\Sigma$,

$$\vec{N}_\Sigma = \begin{vmatrix} \vec{i} & \vec{j} & \vec{k} \\ \dot{X}_u & \dot{Y}_u & \dot{Z}_u \\ \dot{X}_\varphi & \dot{Y}_\varphi & \dot{Z}_\varphi \end{vmatrix}, \tag{35}$$

Table 3

Errors of the characteristic curve / *Erori pe curba caracteristică*

AB				BC			
X	Y	Z	C	X	Y	Z	C
-0.0446	0.8732	-0.6259	4.6207e-005	-0.0446	0.8732	-0.6259	4.6207e-005
-0.0520	0.8261	-0.5695	1.5153e-005	-0.0520	0.8261	-0.5695	1.5153e-005
-0.0598	0.7793	-0.5128	-6.6328e-005	-0.0598	0.7793	-0.5128	-6.6328e-005
-0.0681	0.7328	-0.4561	-3.7875e-005	-0.0681	0.7328	-0.4561	-3.7875e-005
-0.0766	0.6867	-0.3992	-8.2799e-005	-0.0766	0.6867	-0.3992	-8.2799e-005
-0.0854	0.6411	-0.3422	-2.6242e-005	-0.0854	0.6411	-0.3422	-2.6242e-005
-0.0942	0.5960	-0.2852	3.1008e-005	-0.0942	0.5960	-0.2852	3.1008e-005
-0.1029	0.5516	-0.2283	7.0897e-005	-0.1029	0.5516	-0.2283	7.0897e-005
-0.1114	0.5080	-0.1714	0.00014249	-0.1114	0.5080	-0.1714	0.00014249
-0.1193	0.4653	-0.1147	7.6904e-005	-0.1193	0.4653	-0.1147	7.6904e-005
CD							
X	Y	Z	C				
0.11933	0.4653	0.11474	7.6904e-005				
0.11135	0.50801	0.17141	0.00014249				
0.10291	0.55162	0.22826	9.1732e-006				
0.09416	0.596	0.28522	8.3885e-005				
0.08534	0.64105	0.34222	8.7694e-005				
0.07661	0.68666	0.39918	1.2563e-005				
0.06804	0.73276	0.45608	6.7785e-005				
0.0598	0.77926	0.51285	3.5996e-005				
0.05196	0.82609	0.56946	1.5153e-005				
0.04464	0.87319	0.62588	-7.4899e-005				

Table 4

Coordinates of axial section of side mill / *Coordonatele secţiunii axiale a sculei disc*

	R [mm]	H [mm]		R [mm]	H [mm]		R [mm]	H [mm]
	4.1309	-0.6000		4.5754	-0.1000		4.5352	0.1500
	4.1768	-0.5501		4.5867	-0.0800		4.4922	0.2000
	4.2227	-0.5000		4.5956	-0.0600		4.4484	0.2500
	4.2684	-0.4500		4.6019	-0.0400		4.404	0.3000
AB	4.3139	-0.4000	**BC**	4.6057	-0.0200	**CD**	4.3592	0.3500
	4.3591	-0.3500		4.6070	0.0000		4.3139	0.4000
	4.404	-0.3000		4.6057	0.0200		4.2684	0.4500
	4.4484	-0.2500		4.6019	0.0400		4.2227	0.5000
	4.4922	-0.2000		4.5956	0.0600		4.1768	0.5500
	4.5352	-0.1500		4.5867	0.0800		4.1309	0.6000

and the position vector, $\vec{r}$.

$$\vec{r} = (X - a)\cdot\vec{i} + Y\cdot\vec{j} + Z\cdot\vec{k}\,, \qquad (36)$$

where *X*, *Y* and *Z* are the coordinates of points from the characteristic curve and *a* is the distance between the side mill axis and helical surface axis.

Next, it was calculated the Nikolaev condition:

$$C = \begin{vmatrix} N_X & N_Y & N_Z \\ A_X & A_Y & A_Z \\ r_X & r_Y & r_Z \end{vmatrix}. \qquad (37)$$

The value of *C* determinant is the error of determination for the characteristic curve. Theoretically, value of the *C* determinant, (37), should be zero.

The values of error in each point are presented in Table 3.

Obviously, the enveloping condition is accomplished for all the points from the characteristic curve, points determined by graphical method. In this way, the capability of the proposed method is proved.

In Figure 10 and Table 4, it is presented the solid model of the revolution surface (the side mill tool) and the coordinates (*R* and *H*) of its axial section.

Obviously, the profiles determined by the two methods, the analytical method and the graphical one, based onto the complementary theorem of the substitutive circles family, are identical.

5. Conclusions

The presented graphical method, developed in CATIA environment, allow a rigorous approach of the issue of axial profile determination for the revolution surface reciprocally enveloping with a composed helical surface. In our case the composed helical surface is the helical flute of the dental bur.

The result of the graphical method was compared with a numerical solution obtained based on a classical analytical method, the Nikolaev theorem.

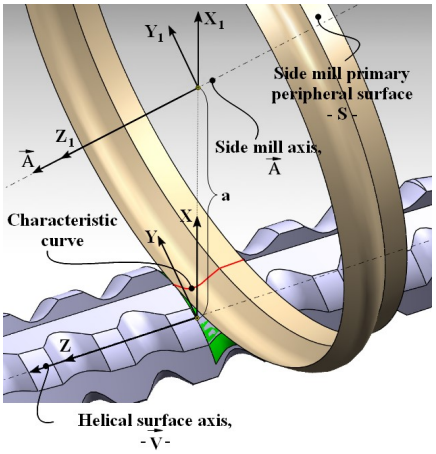

Fig. 10 - Solid model of the side mill – *S* / *Modelul solid al suprafeţei de revoluţie (scula disc)*.

The graphical method is fast, very rigorous and, in the same time, intuitive.

By these characteristics, the method allows, easily, profiling a secondary order tool with form optimized for generating various geometries of the helical flutes customized for materials used for modern dental crowns, especially considering: ceramic materials; metalo-ceramic; porcelain; acrylate and composite materials.

The graphical method principle can be applied for others tools bounded by revolution primary peripheral surfaces: end mill tool or ring tool.

Using the soft suites for computer assisted design, may allows, besides design, the simulation of the working conditions at machining any specified material, in order to study the temperature in working zone, with possibility to change the cutting one geometry, with goal to obtain tools with optimized geometry.

REFERENCES

1. H. Sein, W. Ahmed, M.J. Jackson, R. Polini, Performance and characterisation of CVD diamond coated, sintered diamond and WC–Co cutting tools for dental and micromachining applications, Thin Solid Films, 2003, **447**.
2. D.F. Galindo, C. Ercoli, P.D. Funkenbusch, T.D. Greene, M.E. Moss, H.J. Lee, U.Ben-Hanan, G.N. Graser, and I. Barzilay, A study on the effect of different variables and a comparison between conventional and channeled diamond burs, Journal of Prosthodontics, 2004, **13**(1), 1.

3. S.C. Siegel, J.A. von Fraunhofer, The cutting efficiency of dental diamond burs: a comparative study, Journal of the American Dental Association, 1996, **127**(6), 763.

4. S. Sharma, R. Shankar, K. Srinivas, An epidemiological study on the selection, usage and disposal of dental burs among the dental practioner's, Journal of Clinical and Diagnostic Research, 2014, **8**(1), 250.

5. L. Hong, L. Zhi, W. Shaojun, Digitization modeling and CNC machining for enveloping surface parts, International Journal of Advanced Manufacturing Technology, 2014, **73**, 209.

6. F.L. Litvin, Theory of gearing. Reference Publication 1212, NASA, Scientific and Technical Information Division, Washington D.C, 1984.

7. V.S. Lukshin, Theory of screw surfaces in cutting tool design, Machinostroyenie, Moscow, 1968.

8. S.P. Radzevich, Kinematic geometry of surface machining, CRC Press, London, New York, 2008.

9. X. Cheng, Z.G. Wang, S. Kohayashi, K. Nakamoto, Tool fabrication system for micro/nano milling. Function analysis and design for six axis wire EDM machine, International Journal of Advanced Manufacturing Technology, 2010, **46**, 176.

10. V.G. Teodor, F. Susac, N. Baroiu, V. Păunoiu, N. Oancea, Graphical method in Catia for side mill tool profiling using the generating relative trajectories, Proceedings of 5th International Conference on Advanced Manufacturing Engineering and Technologies - NEWTECH, Belgrade, 2017, edited by V. Majstorovic, Z. Jakovljevic (Springer International Publishing AG, 2017), p. 215.

11. N. Baroiu, S. Berbinschi, V.G. Teodor, F. Susac, N. Oancea, The complementary graphical method used for profiling side mill for generation of helical surface, ModTech International Conference Modern Technologies in Industrial Engineering (Modtech 2017), IOP Conf. Series: Materials Science and Engineering, **227**, Article Number: 012013.

12. N. Oancea, Generarea suprafeţelor prin înfăşurare (Surfaces generation by enwrapping) Vol. II, Teoreme complementare, Editura Fundaţiei Universitare „Dunărea de Jos" - Galaţi, 2004.

13. G. Frumuşanu, N. Oancea, Technological solution to profile and generate the teeth of central gear precession gear drives, International Journal of Advanced Manufacturing Technology, 2012, **67** (14), 687.

14. G. Frumuşanu, S. Berbinschi, N. Oancea, The ring-tool profiling in Catia graphical environment, based on the family of substituting circles method, Applied Mechanics and Materials, 2014, **656**, 137.

****

SCIENTIFIC EVENTS

6th International Conference on Smart Materials & Structures
April 16-17, 2018 Las Vegas, Nevada, USA
Theme: Rise of a Smart Materials and Structures era

Smart Materials & Structures 2018 defines various fields of research like Bio materials, Nano materials, Nano technology, Mechanical & Aerospace engineering, Chemical analysis in Biochemistry, Smart Polymeric materials, Ceramics smart materials, Smart materials for healthcare etc.

Track 1: Smart Materials and Technologies
Track 2: Smart Structures
Track 3: Optical and Electronic Materials
Track 4: Materials for Energy Conversion and Storage
Track 5: Nano materials and Nanotechnology
Track 6: Smart Biomaterials
Track 7: Mechanics and Behavior of Smart Materials
Track 8: Architecture and Civil Engineering
Track 9: Material Chemistry
Track 10: Smart Grid Technology

Contact: https://smartmaterials-structures.conferenceseries.com/

****